

Coupled resonator-induced transparency on a three-ring resonator

Xinquan Jiao(焦新泉), Haobo Yu(于皓博), Miao Yu(于淼), Chenyang Xue(薛晨阳), Yongfeng Ren(任勇峰)
Citation: Chin. Phys. B . 2018, 27(7): 074212. **doi:** 10.1088/1674-1056/27/7/074212

Journal homepage: http://cpb.iphy.ac.cn; http://iopscience.iop.org/cpb

What follows is a list of articles you may be interested in

Geometrical representation of coherent tunneling process in two-waveguide and three-waveguide coupler

Jian Shi(时坚), Rui-Qiong Ma(马瑞琼), Zuo-Liang Duan(段作梁), Meng Liang(梁猛), Bao-Yu Chai(柴宝玉), Jun Dong(董军)
Chin. Phys. B . 2017, 26(12): 124214. **doi:** 10.1088/1674-1056/26/12/124214

Silica-based microcavity fabricated by wet etching

H Long(龙浩), W Yang(杨文), L Y Ying(应磊莹), B P Zhang(张保平)
Chin. Phys. B . 2017, 26(5): 054211. **doi:** 10.1088/1674-1056/26/5/054211

Coupled-resonator-induced transparency in two microspheres as the element of angular velocity sensing

Kun Qian(钱坤), Jun Tang(唐军), Hao Guo(郭浩), Wei Zhang(张伟), Jian-Hua Liu(刘建华), Jun Liu(刘俊), Chen-Yang Xue(薛晨阳), Wen-Dong Zhang(张文栋)
Chin. Phys. B . 2016, 25(11): 114209. **doi:** 10.1088/1674-1056/25/11/114209

Plasmon resonance coupling in strongly coupled gold nanotube arrays with structural defects

Zhou Xin, Fang Jian-Shu, Yang Di-Wu, Liao Xiang-Ping
Chin. Phys. B . 2012, 21(8): 084202. **doi:** 10.1088/1674-1056/21/8/084202

Modeling and analysis of silicon-on-insulator elliptical microring resonators for future high-density integrated photonic circuits

Xiong Kang, Xiao Xi, Hu Ying-Tao, Li Zhi-Yong, Chu Tao, Yu Yu-De, Yu Jin-Zhong
Chin. Phys. B . 2012, 21(7): 074203. **doi:** 10.1088/1674-1056/21/7/074203

Coupled resonator-induced transparency on a three-ring resonator*

Xinquan Jiao(焦新泉)[1,2,†], Haobo Yu(于皓博)[1,2], Miao Yu(于淼)[1,2],
Chenyang Xue(薛晨阳)[1,2], and Yongfeng Ren(任勇峰)[1,2]

[1] *Science and Technology on Electronic Test and Measurement Laboratory, North University of China, Taiyuan* 030051,*China*
[2] *Key Laboratory of Instrumentation Science & Dynamic Measurement (Ministry of Education), North University of China, Taiyuan* 030051, *China*

(Received 9 February 2018; revised manuscript received 30 March 2018; published online 25 June 2018)

The coupled resonator-induced transparency (CRIT) phenomenon, which is analogous to electromagnetically induced transparency in atomic systems, can occur in an original integrated optical resonator system due to the coherent interference of the coupled optical resonators. The system was composed of three ring resonators on silicon, each with the same cavity size, and the optical coupling to the input and output ports was achieved using grating with a power coupling efficiency of 36%. A CRIT resonance whose spectrum shows a narrow transparency peak with a low group velocity was demonstrated. The quality factor of the ring resonator can attain a value up to 6×10^4, and the harmonic wavelength can be controlled by adjusting the temperature. The through and drop transmission spectra of the resonator are reconciled well with each other and also consistent well with the theoretical analysis.

Keywords: coupled resonator-induced transparency, three-ring resonator, coupling efficiency, transmission spectra, quality factor

PACS: 42.60.Da, 42.82.Et, 42.60.Lh **DOI:** 10.1088/1674-1056/27/7/074212

1. Introduction

Recent findings have indicated that the phenomena analogous to electromagnetically induced transparency (EIT) in atomic systems can also be found in whispering-gallery mode resonators, commonly termed as coupled resonator-induced transparency (CRIT).[1] In contrast to EIT in atomic systems, CRIT is based on structural dispersion. Thus, the CRIT system has many advantages: the available frequencies are not restricted to intrinsic atomic transitions and the system has flexibility in terms of the design space and is free from the Doppler effect.[2] In a coupled resonant cavity,[3–5] mutually independent resonant states interact via the weak coupling effect between different cavities, thus changing the characteristics of the entire resonant system and generating coupled resonator-induced transparency.[6] Their characteristics and potential for use in complex and flexible configurations make these devices particularly attractive for integrated optics or various applications in optical precursors, such as optical sensing,[7,8] the feedback cavity of a laser,[9] optical filters,[10,11] and so on. The CRIT effect of a resonator has a significant relationship with the coupler insertion loss, the ring circumference, and the multiples of the rings.[12,13]

In fact, CRIT mainly involves the control of the optical resonator to reduce the resonance interference between the optical circuit and the precise perimeter difference between coupled resonant cavities.[14] In the structure design and preparation process, controlling the resonator's perimeter difference requires an accurate complex calculation process with advanced process requirements. So far, it is common to report on CRIT double-ring resonators, such as a silicon dual-coupled-ring resonator modulator based on push–pull coupling tunings,[15] a silicon thermo-optic switch based on dual-ring resonators,[16] a ring-in-ring structure resonator,[17] and so on. The multi-ring structure is basically in the theoretical research stage, and the design, preparation, and testing of a specific three-ring structure have not been reported.[18] In this paper, we proposed a new three-ring cascade resonator structure with the same cavity size which does not require precise calculation of the perimeter between the resonator cavities compared with other cascade structures, thereby greatly reducing the difficulty of design and preparation. In addition, because of multiple passes in the cavity, the structure could obtain a high Q factor and provide a significant delay in the time of light travel. The new three-ring cascade resonator is significant for the optimization of the design of a micro-ring resonator structure, the improvement of coupled resonator-induced effects, and the shortening of the preparation period.

2. Theoretical analysis

Figure 1(a) shows the schematic illustration of the coupled three-ring resonators. Figure 1(b) is a scanning-electron micrograph of a three-ring resonator in this scheme. All three micro-ring resonators are identical in geometry and have center resonance wavelengths represented by λ_1, λ_2, and λ_3 ($\lambda_3 \neq \lambda_2 \neq \lambda_3$), respectively. g_n is the gap between the micro-ring resonators, and g is the gap between the bus waveguides and the micro-ring resonators. k^2 is the power coupling coefficient between the bus waveguides and the micro-ring resonators, and k_n^2 is the mutual power coupling coefficient between the micro-ring resonators. The propagation power loss coefficient is k_p^2 per round-trip in each micro-ring resonator.

*Project supported by the National Natural Science Foundation of China (Grant Nos. 61771434, 91123036, 61178058, 61275166, and 61076111) and the National Science Fund for Distinguished Young Scholars, China (Grant No. 51225504).

†Corresponding author. E-mail: jiaoxinquan@nuc.edu.cn

© 2018 Chinese Physical Society and IOP Publishing Ltd

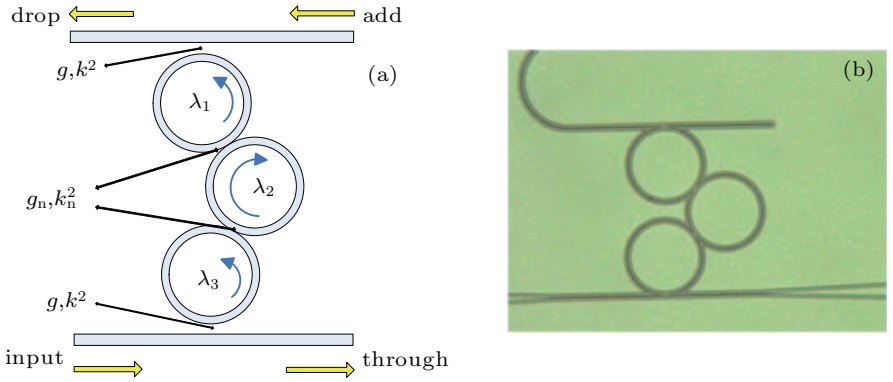


Fig. 1. (color online) (a) Schematic illustration of a three-order coupled micro-ring resonator. (b) Scanning-electron micrograph of the three-ring resonator.

With the development of coupled-mode-theory (CMT), it can be shown that the add-drop response in the wavelength-domain parameters of a three-order micro-ring filter can be obtained by solving the following matrix equation:

$$\begin{bmatrix} -\mathrm{j}\dfrac{\lambda-\lambda_1}{FSR}+\dfrac{\left(k^2+k_\mathrm{p}^2\right)}{4\pi} & \mathrm{j}\dfrac{k_\mathrm{n}}{2\pi} & 0 \\ \mathrm{j}\dfrac{k_m}{2\pi} & -\mathrm{j}\dfrac{\lambda-\lambda_2}{FSR}+\dfrac{k_\mathrm{p}^2}{4\pi} & \mathrm{j}\dfrac{k_\mathrm{n}}{2\pi} \\ 0 & \mathrm{j}\dfrac{k_\mathrm{n}}{2\pi} & -\mathrm{j}\dfrac{\lambda-\lambda_3}{FSR}+\dfrac{\left(k^2+k_\mathrm{p}^2\right)}{4\pi} \end{bmatrix} \times \begin{bmatrix} s_1 \\ s_2 \\ s_3 \end{bmatrix} = \begin{bmatrix} \dfrac{k^2}{2\pi} \\ 0 \\ 0 \end{bmatrix}, \tag{1}$$

where s_1, s_2, and s_3 represent the normalized complex wave field in a lumped coupled resonator system. The complex amplitude transmission is then expressed by $T_\mathrm{through} = 1 - S_1$ and $T_\mathrm{drop} = -S_3$ for the through port and the drop port, respectively. The corresponding power transmissions for the through port and the drop port are $\left|T_\mathrm{through}\right|^2$ and $\left|T_\mathrm{drop}\right|^2$, respectively.

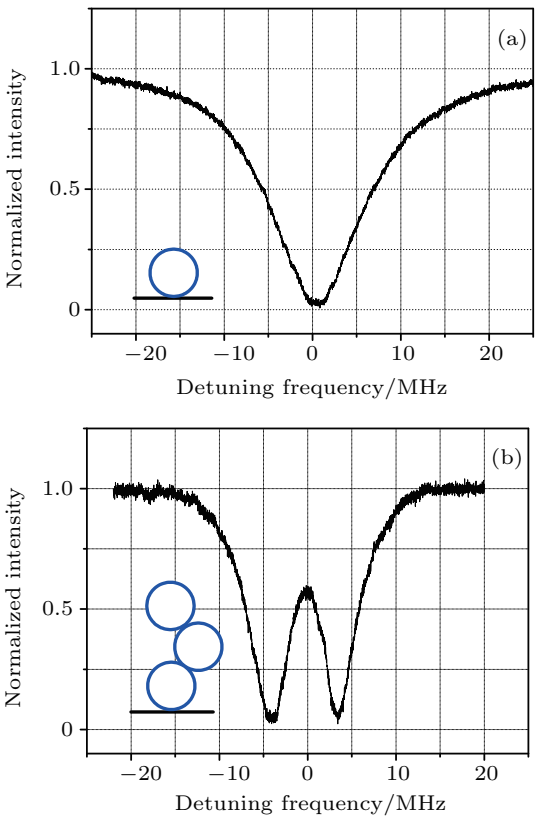


Fig. 2. (color online) Transmission spectra as a function of the detuning frequency from resonance (a) through a single-ring resonator and (b) through a three-ring resonator.

For applications in telecommunications, the time behavior of the micro-ring, or alternatively the frequency response to a time-varying signal, is of great importance. Since the filter is a resonant filter, the delay depends on the frequency (wavelength) with respect to the resonance. This dependence can be conveniently described by the structural or quadratic dispersion D. This dispersion is the second derivative of the transmission phase-response $\varphi(\omega)$ with respect to the frequency. The normalized group delay τ_n is the negative derivative of the phase-response, with T being the inverse of the FSR:

$$\tau_\mathrm{n} = -\frac{\mathrm{d}}{\mathrm{d}w}\varphi(\omega), \tag{2}$$

$$D = -c\frac{T}{\lambda^2}\frac{\mathrm{d}}{\mathrm{d}\omega}\tau_\mathrm{g}(\omega). \tag{3}$$

Figure 2(a) is the transmission spectrum of a single-ring resonator. In Fig. 2(b), the dip in the transmission spectrum of the single-ring resonator arises due to the destructive interference between the two optical pathways. We consider this dip to be an example of CRIT.[19]

3. Fabrication and test

When the waveguide width is less than 600 nm, the transmission waveguide is of the single-mode type, which can effectively reduce the transmission loss. With the increase in the

width of the silicon-based optical waveguide, the effective refractive index increases, while the intensity of the evanescent wave in the light field is inversely proportional to the width of the waveguide.[20] In addition, the width of the waveguide is proportional to the effective refractive index of the bended waveguide, and the effective refractive index and the size of the bending radius are also closely related. The relationship between the effective refractive index and the bending radius can be obtained by using the beam propagation method (BPM), as shown in Fig. 3. Through the comprehensive consideration of the theory and technology, we chose the waveguide width to be 500 nm and the annular cavity radius to be 20 μm to increase the near-field coupling between the straight waveguide and the annular cavity, thereby effectively reducing the bending losses of the annular cavity.

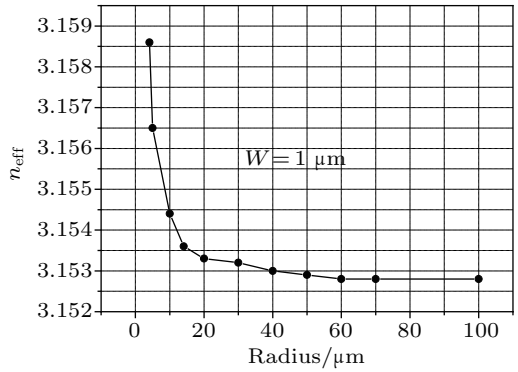


Fig. 3. The effective refractive index versus bending radius diagram by using the beam propagation method.

Our devices were fabricated on a SOI wafer with a top silicon layer thickness of 220 nm and a buried oxide thickness of 1 μm. The optical waveguides and optical ring resonator were fabricated in two steps. First, the positive photo-resist of PMMA was spun on the SOI wafer and the pattern was written using an electron-beam lithography (EBL) system via exposure of the relevant regions using a 100-kV electron beam. The residual photo-resist in the exposure area was removed, and then, the developed graphic was used as a mask for dry etching. Second, inductively coupled-plasma (ICP) reactive-ion-etch (RIE) was used to transfer the pattern and etch through the 220-nm silicon layer.[21]

The top-view microscope image of the fabricated device is shown in Fig. 4. Figures 4(a) and 4(b) are the electron scanning diagrams of the single-ring resonator and the three-ring resonator, respectively, and the preparation process is exactly the same. The device consists of a three-ring resonator with a diameter of 20 μm coupled to a pair of parallel silicon strip waveguides. The waveguides and the rings have widths of 500 nm and 600 nm, respectively, and the distance between the straight waveguide and the rings is 129 nm, with the rings being tangent to each other.

The test platform was set up as shown in Fig. 5. The optical signal is generated from a New Focus tunable laser with 1550 nm center wave length, and the laser is connected to an erbium-doped fiber amplifier (EDFA) with a magnification of 50 times. A polarization controller is used before the input of the single-mode optical fiber lens with 10.4 μm diameter coupled to the waveguide to study the effects of different polarization states on the laser coupling efficiency of the grating. The silicon waveguide grating enables the vertical coupling of light into the SOI system; after transmission through the device, light is transferred to another vertical grating coupler to recover the light to the output of the single mode lens fiber.[22]

During the test, a precise three-dimensional adjustable frame with adjustable accuracy of 2 nm was used to fix the input and the output single-mode optical fibers, and the sample was aligned and fixed relative to these fibers by using an infrared CCD and a long focal distance microscope. Using this setup, we could continuously monitor the optical route, thereby easily performing the alignment of the single-mode fiber gratings.[23] The optical signal was converted to an electrical signal by using a photoelectric converter, and then the electrical signal was shown on an oscilloscope after being amplified by a signal amplifier. By repeating the test as shown in Fig. 6, we obtained a grating coupler efficiency of 30% at the wavelength of 1550 nm. After spin coating a uniform 500-nm thick antireflection film onto the grating surface, the coupling efficiency was improved to 36%.

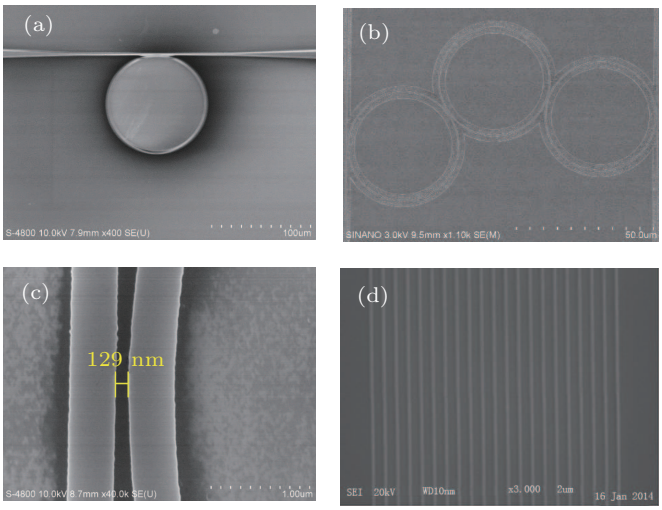


Fig. 4. Scanning-electron micrographs of (a) a single-ring resonator, (b) a three-ring resonator, (c) gap of 129 nm between the bus waveguide and ring resonator, (d) nano-wave guide gratings.

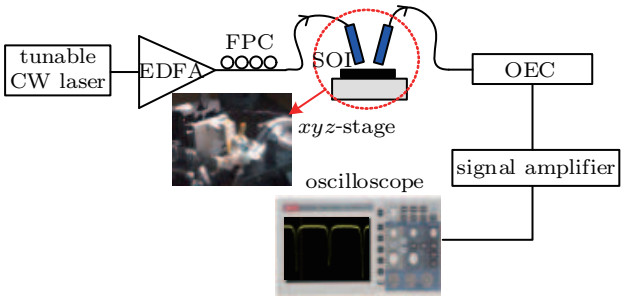


Fig. 5. (color online) Schematic of the test platform.

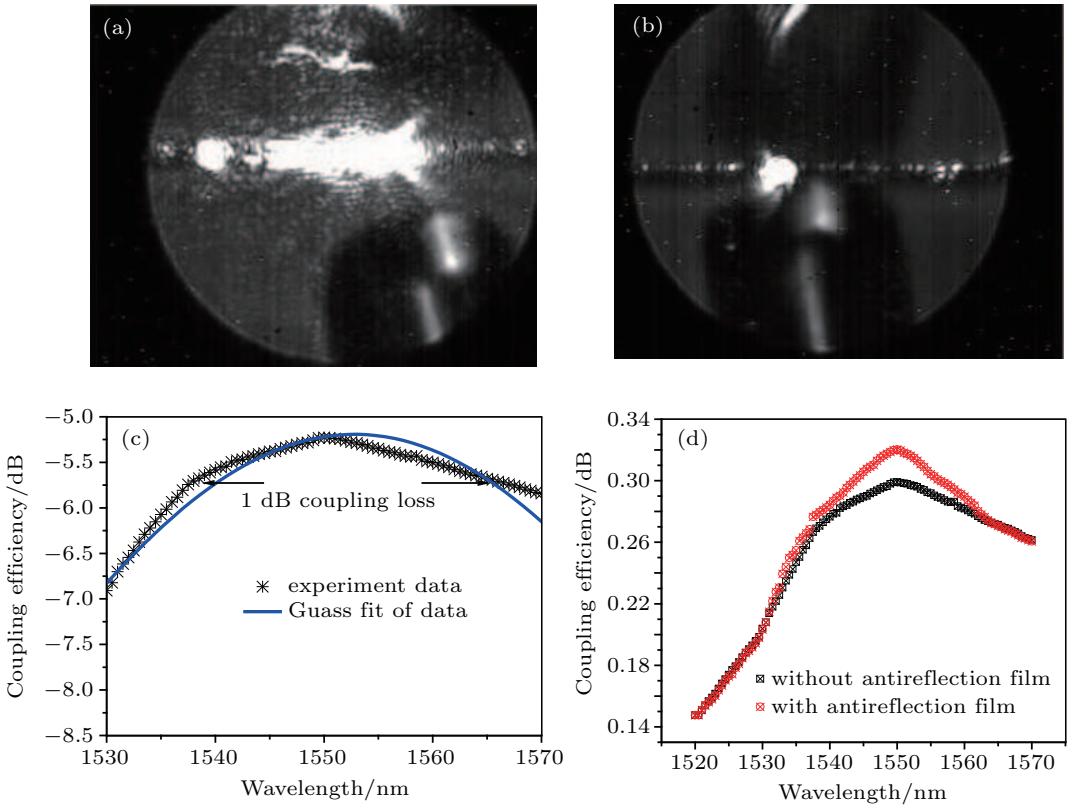


Fig. 6. (color online) (a) Vertical nano-grating coupled input renderings, (b) output renderings, (c) test result curve, (d) comparing the test results of coupling efficiency.

We used the platform to test the coupling induced transparency effect of the coupled three-ring resonators.[24] The resonant peak of the single-ring resonator is observed to split into two. The result presents a high-Q resonant mode when the low-Q resonances of all ring resonators couple coherently. Figure 7 shows the transmission spectra of two types of quasi-TE modes of the device structure, where the red spectrum denotes the response of a single-ring structure and the black spectrum denotes the response of the three-ring cascade structure. When the three-ring resonators are out of resonance, light passes through the waveguide without coupling with the ring resonators, and the transmission is high at this moment. When light is coupled into one of the ring resonators, the resonator acts like a mirror reflecting the light from one ring resonator into another. As seen from Fig. 7(b), due to the mutual interference between the annular cavities of the three-ring resonators, which produces two transmission peaks, one of the half-high widths of the resonance peaks is 0.0264 nm, corresponding to the quality factor Q being as high as 6×10^4, which is four times higher than that of the single-ring structure. The through and drop transmission spectra of the resonator are reconciled well with each other. These results are of great significance for the silicon sensing field. It is worth noting that a very small peak also appears on the single-ring transmission line in Fig. 7(b). The peak is a kind of noise, which is caused by the light path noise (such as scattering noise, polarization noise, etc.) and circuit noise in the test platform, but not the coupled resonator-induced transparency (CRIT) mentioned in this paper.

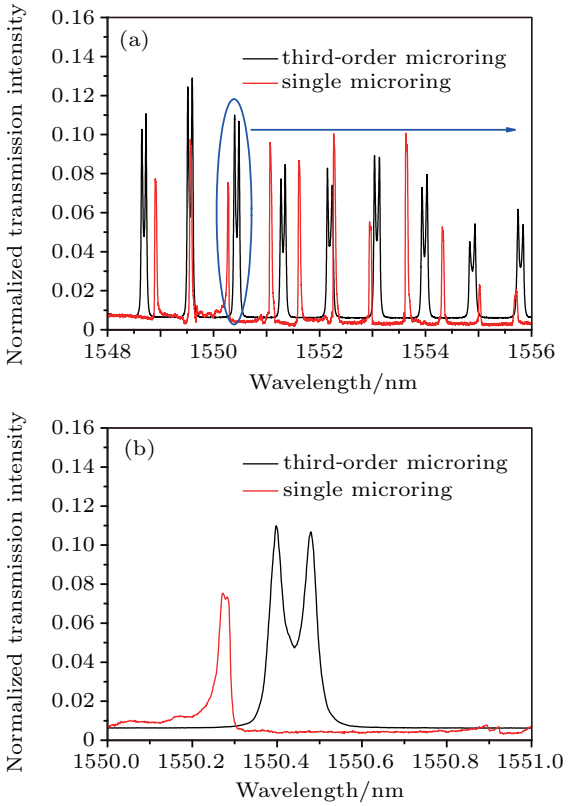


Fig. 7. (color online) Drop transmission spectra of single-ring and three-ring resonators. Panel (b) is partly enlarged view of (a).

Since the resonator produces optical power loss, some of the power of loss is converted into heat energy, and the temperature of the resonator is raised, thus affecting the refractive index of the waveguide medium.[25] This change will cause the drift of the resonant frequency, which will change the performance of the device. In order to obtain the sensitivity of the cascaded ring resonator to the temperature, a temperature tuning experiment was carried out on the resonator of the three-ring cascade structure. The test results are shown in Fig. 8, and the curves of different colors represent different temperatures of the resonance line. As can be seen from Fig. 8, the resonant peak of this structure moves towards the direction of the large wavelength with the increase of temperature, namely, the phenomenon of red shift occurs. Through calculation and analysis of the three-ring cascade resonator with temperature changing in the relation of 0.16 nm/°C, the detuning of the resonance wavelength could be controlled by changing the temperature.

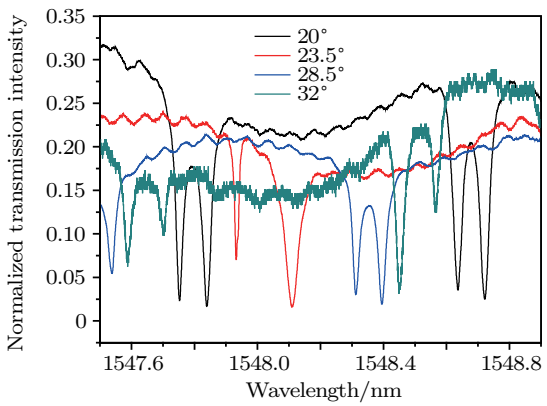


Fig. 8. (color online) Three-ring cascade resonator temperature detuned spectrum.

4. Conclusion

We analyzed the theory of an original three-ring resonator and described the preparation process. The samples were tested and analyzed, and the obtained coupling efficiency and quality factor, along with the observation of CRIT, were well validated. Compared with double-ring resonators in previous reports (the transmission of the double-ring shows a dip with a full width at half maximum of 0.077 nm, corresponding to a quality factor of $Q = 20000$[26]), the quality factor of the three-ring resonators is three times higher than that of the double-ring resonators, and the bandwidth is narrower. At the same time, on the basis of ensuring the coupling efficiency and quality factor, the structure can efficiently reduce the difficulty of design and preparation, which has a good feasibility. In summary, this system has many advantages and is suitable for the systematic and precise study of fundamental physics and for various applications of optical precursors.

References

[1] Smith D D, Chang H, Fuller K A, Rosenberger A and Boyd R W 2004 *Phys. Rev. A* **69** 063804
[2] Oishi T, Suzuki R, Sultana P and Tomita M 2012 *Opt. Lett.* **37** 2964
[3] Xu Q, Sandhu S, Povinelli M L, Shakya J, Fan S and Lipson M 2006 *Phys. Rev. Lett.* **96** 123901
[4] Xu Q, Shakya J and Lipson M 2006 *Opt. Express* **14** 6463
[5] Totsuka K, Kobayashi N and Tomita M 2007 *Phys. Rev. Lett.* **98** 213904
[6] Naweed A, Farca G, Shopova S I and Rosenberger A T 2005 *Phys. Rev. A* **71** 043804
[7] Little B E, Chu S T, Haus H A, Foresi J and Laine J P 1997 *J. Lightw. Technol.* **15** 998
[8] Amemiya Y, Tokunaga T, Tanushi Y and Yokoyama S 2009 *Opt. Rev.* **16** 247
[9] Yanik M F and Fan S 2004 *Phys. Rev. Lett.* **92** 083901
[10] Mancinelli M, Borghi M, Bettotti P, Fedeli J M and Pavesi L 2013 *J. Lightw. Technol.* **31** 2340
[11] Ang T Y and Ngo N Q 2012 *J. Opt. Soc. Am. B* **29** 1094
[12] Wang N, Zhang Y D and Yuan P 2011 *Chin. Phys. B* **20** 044203
[13] Li Z Q, Bai L D, Gu E D, Xie R J, Liu T L, Niu L Y and Feng D D 2017 *Acta Phys. Sin.* **20** 204203 (in Chinese)
[14] Zhang Y D, Wang N, Tian H, Wang H, Qiu W, Wang J F and Yuan P 2008 *Phys. Lett. A* **372** 5848
[15] Zhou Z and Feng L S 2017 *IEEE Photon. J.* **99** 6600112
[16] Zhu Q M, Jiang X H, Yu Y P, Cao R Y, Zhang H X, Li D P and Li Y B 2018 *IEEE Photon. J.* **1** 6600311
[17] Xu X H, Chen Y Q, Guo Z W and Miao X Y 2018 *Acta Phys. Sin.* **2** 024210 (in Chinese)
[18] Jiao X Q, Chen J B and Wang X L 2015 *Acta Phys. Sin.* **14** 144202 (in Chinese)
[19] Totsuka K and Tomita M 2007 *Opt. Lett.* **32** 3197
[20] Chen T, Lee H, Li J, Painter O and Vahala K J 2012 *Nat. Commun.* **3** 867
[21] Tang Y H, Lin Y H, Chen P L, Shiao M H and Hsiao C N 2014 *Micro & Nano Lett.* **9** 395
[22] Xiao S J, Khan M H, Shen H and Qi M H 2007 *Opt. Express* **15** 10553
[23] Vlasov Y and Mcnab S 2004 *Opt. Express* **12** 1622
[24] Maleki L, Matsko A B, Savchenkov A A and Ilchenko V S 2004 *Opt. Lett.* **29** 626
[25] Liu Y, Sun Y, Yi Y J, Tian L, Cao Y, Chen C M, Sun X Q and Zhang D M 2017 *Chin. Phys. B* **26** 124215
[26] Cui D F, Wei L P, Liu C and Liu Y Y 2013 *Micro & Nano Lett.* **10** 619